Scientific Reports

https://doi.org/10.1038/s41598-026-39802-y

Article in Press

Mechanism and engineering practice of roof stability for secondary gob-side entry retaining in deep mines

Received: 6 January 2026

Accepted: 9 February 2026

Published online: 18 February 2026

Cite this article as: Wu J., Chen J. & Xie F. Mechanism and engineering practice of roof stability for secondary gob-side entry retaining in deep mines. *Sci Rep* (2026). https://doi.org/10.1038/s41598-026-39802-y

Jingke Wu, Jiarui Chen & Fuxing Xie

Mechanism and engineering practice of roof stability for secondary gob-side entry retaining in deep mines

Jingke Wu[1]✉, Jiarui Chen[2] ✉ Fuxing Xie[3]

[1]School of Intelligent Manufacturing and Smart Transportation, Suzhou City University, Suzhou 215104, China.
[2]Faculty of Architecture and Civil Engineering, Huaiyin Institute of Technology, Huai'an 223001, China.
[3]Beijing China Coal Mine Engineering Co., Ltd., Beijing 100013, China.
✉email: jkwucumt@126.com

To facilitate the reuse of the gob-side retained entry as a long-term return airway, alleviate mining-excavation pressure, and reduce roadway development costs, this paper proposes a secondary gob-side entry retaining technique. The study examines the movement behavior of overlying strata throughout the entire process of secondary gob-side entry retaining, introduces a roof support concept based on “major and minor structural zones,” establishes a mechanical model of the roof structure for secondary retention, derives a design formula for the roadside backfill, analyzes the main factors influencing the stability of the overlying strata structure, and proposes an integrated “four-in-one” surrounding rock control technology for secondary gob-side entry retaining. The results indicate that: (1) The “major structural zone” of the overlying strata stabilizes only after experiencing three mining disturbances. (2) The coordinated load-bearing behavior of the “minor structural zone” in roof support is crucial to surrounding rock stability. A “four-in-one” control strategy is proposed, integrating the roadside packing bodies on both sides, the roof bolting-cable system, floor reinforcement, and internal roadway support to form a stable load-bearing structure. (3) Appropriately reducing the roadway width, the widths of the two packing bodies, and the cantilever length of the main roof on the goaf side can enhance the support capacity of the coal rib during the initial retention stage. This reduces the load on the packing bodies during the secondary gob-side entry retaining stage, thereby alleviating surrounding rock stress. The proposed approach has yielded favorable outcomes in engineering practice, demonstrating both theoretical relevance and practical significance for supporting roadways under similar conditions.

Keywords Deep mine, Secondary gob-side entry retaining, Roof, Surrounding rock, Backfill

1.Introduction

Gob-side entry retaining is a technique that preserves the mining gateway behind the active longwall face for reuse as an access roadway in adjacent panels [1, 2], as illustrated in Figure 1(a). To date, significant progress has been made in GER technology in China, especially for thin to medium-thick coal seams under favorable geological conditions [4]. Related supporting techniques—such as roadside support, in-roadway reinforcement, and coal rib strengthening—have reached a relatively mature stage of development [3, 5]. To maintain the retained entry as a permanent return air channel during the mining of subsequent adjacent panels, this study proposes a secondary gob-side entry retaining method based on existing surrounding rock control theories and practices. This approach involves constructing a second backfill

wall along the goaf edge behind the adjacent working face, ultimately forming a roadway enclosed by two backfill walls with the preserved passage in between, as shown in Figure 1(b). The secondary gob-side entry retaining technique serves two main purposes: Enabling "Y-type" ventilation for adjacent high-gas panels [6]; Maintaining the roadway as a long-term, multi-purpose return air channel, thereby achieving the concept of "multi-functional roadway utilization." Moreover, this method holds considerable theoretical and practical significance in reducing roadway development costs, mitigating mining–excavation coordination conflicts, and eliminating the need for isolated working faces.

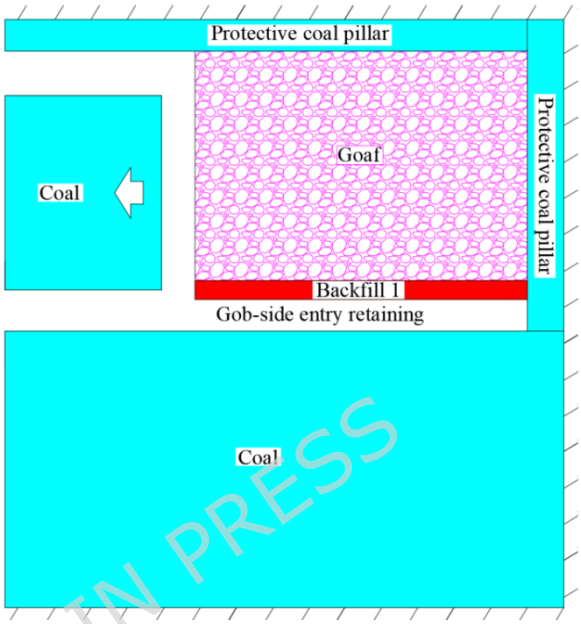

(a) Gob-side entry retaining

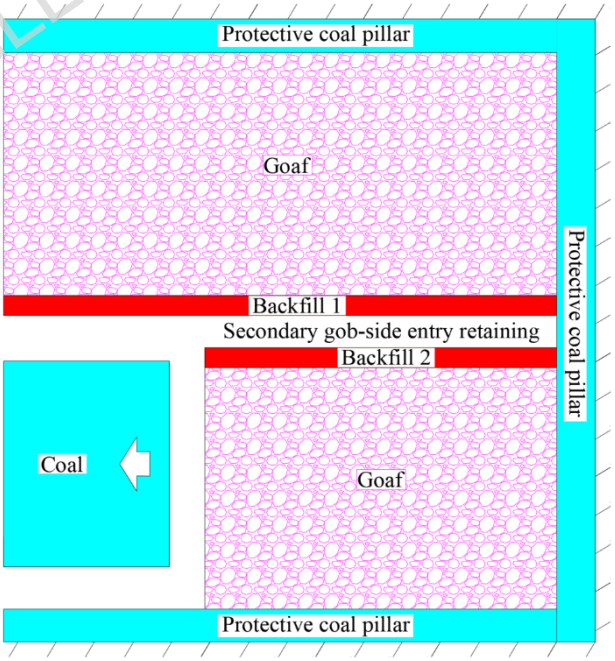

(b) Secondary gob-side entry retaining

Fig. 1. Schematic diagram of roadway layout in coal mining face.

Currently, research on the theory and application of secondary gob-side entry retaining remains limited, particularly in terms of integrated control systems and long-term stability under multiple mining disturbances. Existing studies have primarily focused on mechanical models of key blocks and fracture positions. For instance, Li established a mechanical model of the key

block for secondary gob-side entry retaining and analyzed the interaction mechanism between the key block and the surrounding rock [7]. Chen developed a structural dmechanical model assuming fracture of the main roof above the coal wall [8], while Kan investigated the influence of different fracture positions, concluding that fractures outside the backfill are most favorable [9].

However, these studies rarely consider the integrated performance of the support system as a whole, and field validation under deep high-stress conditions is scarce. To address these gaps, this paper proposes a novel “four-in-one” surrounding rock control methodology, establishes a refined mechanical model for secondary gob-side entry retaining considering both major and minor structural zones, and validates the proposed model and methodology through extensive field monitoring in a deep coal mine.

2.Activity Laws of Overlying Strata above Secondary Gob-Side Entry Retaining

The “large structure” of roadway refers to the key block system formed by the fractured main roof above the goaf, which undergoes successive adjustments due to mining disturbances. The “small structure” comprises the roadway roof, two backfill bodies, internal supports, and floor, which directly bear and transfer loads to maintain local stability. The stability of key blocks at the coal face end depends on the fracture location within the lateral main roof of the stope. Furthermore, the positions of main roof fractures in gob-side entry retaining significantly affect the surrounding rock behavior in secondary gob-side entry retaining, ultimately determining the stability of the key blocks in the main roof during the secondary gob-side entry retaining stage. Therefore, this section first analyzes the fracture positions of key blocks above the end of the gob-side entry retaining, followed by a stability analysis of the key blocks in the main roof under secondary gob-side entry retaining conditions.

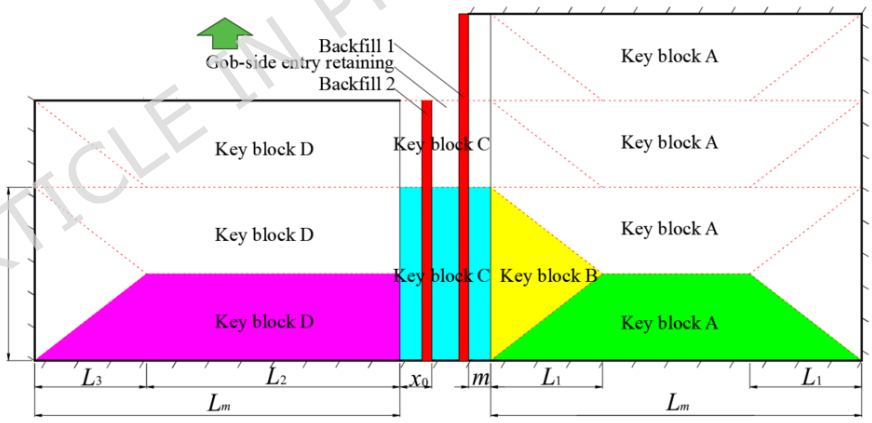

Fig. 2. Schematic diagram of basic top fracture between adjacent working faces.

As mining advanced in the upper-section coal face, the main roof above the goaf gradually evolved into a state of being clamped at four ends. The first weighting event led to the formation of an “O-X” type fracture. Subsequent periodic weighting consistently produced a “semi-O-X” type fracture pattern in the main roof over the goaf [10, 11], as shown in Figure 2. During the gob-side entry retaining process, the initial fracture of the main roof and the lower rock strata occurred outside backfill 1. In this scenario, the roadway was located beneath the end section of key block C within the intact main roof. Key blocks C, A, and B articulated with each other, forming a “large structure” [12], as illustrated in Figure 3(a). When the roof cutting height of backfill 1 reached a certain level and could no longer propagate upward, a second fracture occurred in the main roof and the lower rock strata, this time above the coal wall adjacent to the roadway [13]. Through the combined support of the backfill, the coal wall beside the roadway, and the immediate roof, key block C articulated with key blocks B and D to form another “large structure”.

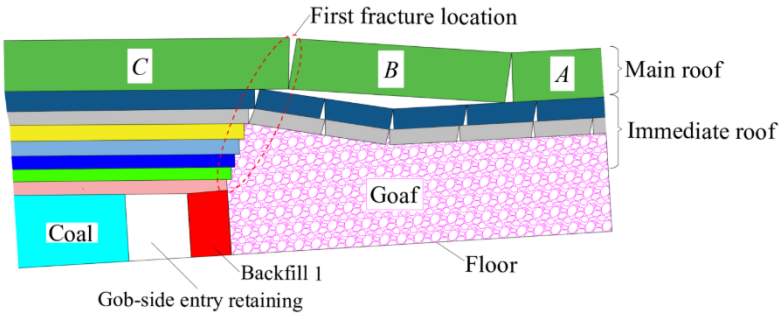

(a) Schematic of the initial roof fracture location for gob-side entry retaining

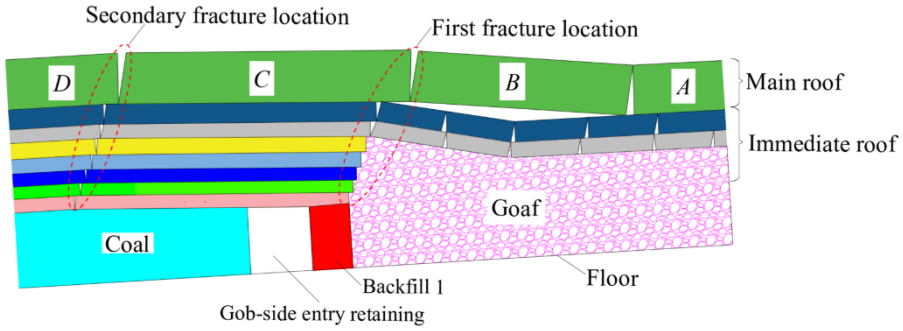

(b) Schematic of the secondary roof fracture location for gob-side entry retaining

Fig. 3. Schematic diagram of the overlying strata fracture structure for the roadway.

During mining in the adjacent lower section, the main roof above the goaf was constrained by intact coal on three sides and supported by a backfill on the fourth side, creating a condition of "three ends clamped and one end simply supported." Under the first weighting, the main roof exhibited an "O-Y" type fracture pattern, and subsequent periodic weighting consistently produced a semi-"O-Y" type fracture pattern [14], as shown in Figure 2. In the secondary gob-side entry retaining stage, the main roof and lower rock strata at the face end were subjected to intense overlying strata activity above the goaf as well as a second fracture in the main roof. A third fracture then formed along the outer edge of backfill 2, whose location may coincide with that of the second fracture in the main roof. The self-weight of key block C and the overlying weak strata were gradually transferred through the immediate roof to backfill 2. Through the coordinated bearing effect of backfill 1, backfill 2, and the immediate roof, key block C articulated again with key blocks B and D to form a "large structure," as illustrated in Figure 4.

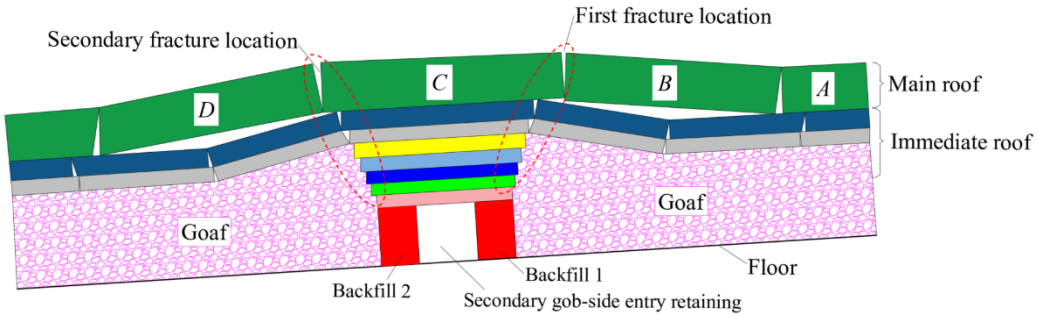

Fig. 4. Schematic diagram of roof fracture structure for secondary gob-side entry retaining.

Based on the preceding analysis, it is evident that the stability of key block C plays a decisive role in maintaining the surrounding rock integrity during the overlying strata activity in secondary gob-side entry retaining. If key block C remains stable after mining in the adjacent upper and lower sections, the stress transferred to the roadway surrounding rock becomes predictable, thereby simplifying the maintenance of the secondary gob-side entry retaining. Conversely, if key block C rotates and sinks into the goaf following mining in the neighboring sections, it will impose substantial dynamic pressure and

induce severe deformation in the roadway support structure, significantly challenging the long-term stability of the secondary gob-side entry retaining.

3. “Small Structure” Stability of Gob-Side Entry Retaining

The “small structure” of the secondary gob-side entry retaining consists of the roadway roof, two backfill bodies, internal roadway supports, and the floor. Its mechanical behavior is influenced by multiple factors, including the geological occurrence, structural characteristics, and redistributed stress field within the lateral rock mass of the goaf, leading to pronounced load asymmetry [15, 16]. As mining proceeds successively in the adjacent upper and lower sections, the deformation and movement of the overlying strata within the “large structure” inevitably affect the stability of the “small structure.” During the transition of the “large structure” from a stable state to a stressed and deformed condition, the capacity of the “small structure” to maintain its integrity becomes a critical factor determining the success of secondary gob-side entry retaining. Consequently, each component of the “small structure” support system must satisfy the required load-bearing capacity.

The “four-in-one” concept integrates four subsystems: two backfills, roof bolting-cable system, floor reinforcement, internal roadway support. They function as a coordinated system: the backfills provide lateral confinement and cut off roof strata; the roof support maintains immediate roof integrity; the floor reinforcement prevents heave and ensures foundation stability; and the internal support redistributes loads and restricts deformation. Together, they form a composite load-bearing structure that balances asymmetrical pressures and minimizes stress concentration.

(1) Load-bearing capacity of the roof

The roof structure in secondary gob-side entry retaining comprises three main components: the roadway roof, the roof over the upper-section backfill [17, 18, 19], and the roof over the lower-section backfill. Each of these significantly affects the stability of the “small structure.” Due to the strong mining influence from both adjacent panels, the roadway roof often exhibits pronounced bed separation, fragmentation, and crack development, making it prone to failure. Therefore, comprehensive support should be applied to all three roof zones, with particular emphasis on the roof above the backfill areas. This not only helps preserve the integrity of the roof strata but also enhances overall support capacity. Meanwhile, during successive mining of the upper and lower sections, measures should be taken to promote the complete caving of the immediate roof and the main roof strata outside the backfill. This reduces the cantilever length of the roof over the roadway, thereby improving stability in both vertical and lateral directions.

(2) Load-bearing capacity of the two filling bodies

Backfills 1 and 2 are integral components of the “small structure” and play a crucial role in maintaining the stability of the roadway surrounding rock [20, 21]. To ensure roadway stability, the backfills must effectively cut off the roof strata at an adequate height, promote their complete collapse, and accommodate roof movement-induced deformation. The performance requirements for the backfills are twofold: Reasonable support parameters. If the initial and final strengths of the backfill are insufficient, it becomes prone to deformation and failure under high mining-induced stress. This reduces its load-bearing capacity, resulting in roof rotation, subsidence, and ultimately the destabilization of the small structure. Conversely, if the backfill is overly stiff and strong but too narrow, the roadway roof may fracture along the inner side of the backfill, causing roof displacement. Alternatively, the backfill may intrude into the floor, leading to severe floor heave. Therefore, appropriate support parameters must be selected to ensure that the backfill performs optimally and improves the stress state of the small structure. Coordinated bearing capacity between the two backfills. The backfills must not only be in close contact with the roof and floor but also coordinate their load-bearing behavior. Failure of one backfill should not trigger progressive failure of the other, as such coordination is essential to prevent the overall instability of the small support structure.

(3) Load-bearing capacity of the support body in the roadway

Roadway support comprises both primary support and auxiliary reinforcement [22, 23]. Primary support typically consists of I-section steel arches, yielding U-steel sets, cable bolts [24, 25], or composite support systems, all intended to control the significant deformation of the surrounding rock. Auxiliary reinforcement is employed when the backfill strength is inadequate during the initial stages of gob-side entry retaining or secondary gob-side entry retaining. This may include single props, timber point props, timber cribs, or specially designed hydraulic supports. Additionally, auxiliary support inside the roadway helps to redistribute forces bidirectionally and effectively restrain floor deformation.

(4) Bearing capacity of the floor

The floor in secondary gob-side entry retaining consists of three interconnected parts: the floor beneath the backfill zone, the roadway floor in the adjacent lower section, and the floor under the backfill zone of the lower section. When the roadway is not influenced by mining, stress concentration in the surrounding rock remains relatively low, and the floor remains stable. Under mining influence, however, high stress induced by overlying strata activity is transmitted through the backfill to the floor. Without proper confinement, the floor becomes prone to heave, resulting in stress release within the shallow floor strata. Therefore, effective floor control is essential for managing roadway surrounding rock deformation, particularly in the backfill zone.

The deformation and failure of the small support structure are spatially non-uniform, and significant deformation or failure in any local component can lead to global instability. To address the specific challenges of secondary gob-side entry retaining, a “four-in-one” control system is proposed for the small support structure, as shown in Figure 5. This integrated approach is designed to achieve the following objectives: (1) Coordinated roof support – ensuring the integrity of the roofs above the upper- and lower-section backfill zones and the roadway roof through synergistic reinforcement. (2) Coordinated roof-floor-backfill interaction – enabling balanced load transfer among the roofs, floors, and backfills in both sections to prevent roof cutting and backfill intrusion into the floor. (3) Coordinated bearing between the two backfills – preventing progressive failure where fracture of one backfill triggers instability in the other. (4) Coordinated interaction between roadway support and backfill – avoiding fracture failure of the backfill during the initial stage of gob-side entry retaining through integrated load-sharing.

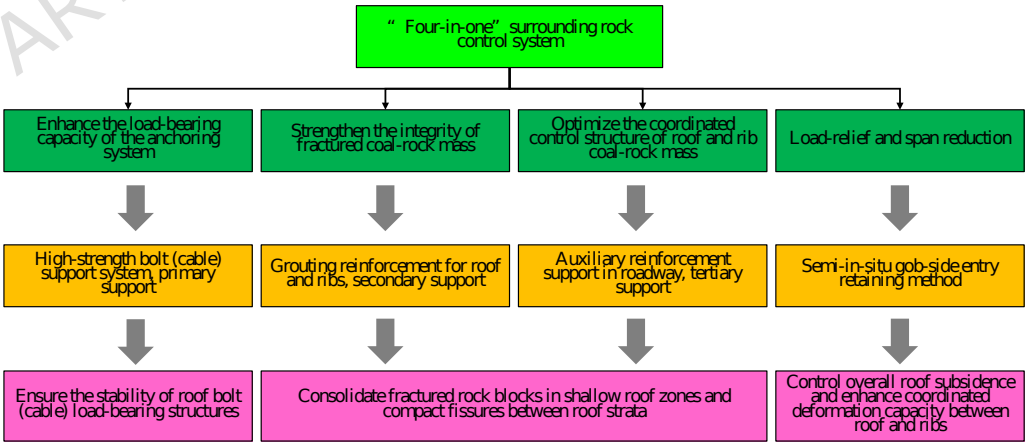

Fig. 5. “Four-in-one” surrounding rock control syestem of secondary gob-side entry retaining.

4. Mechanical Analysis of Surrounding Rock Stability for Secondary Gob-Side Entry Retaining

From an engineering perspective, the stability analysis of surrounding rock in secondary gob-side entry retaining focuses on the most critical cross-section during the most hazardous stage of strata movement. Based on the temporal evolution of roof activity in gob-side entry retaining, Sun et al. [1] classified the process into three phases: early, transitional, and late periods, and

established a corresponding mechanical model using a laminated plate theory. Feng [26] elucidated the role of the roadway-side backfill at each stage of roof movement and derived a mathematical model for support resistance. Jia and Liu [27, 28] developed a mechanical model for gob-side entry retaining with cemented paste backfill and proposed a method for determining the key parameters of the roadside support. Building on these previous studies, this paper establishes a composite laminated mechanical model that reflects the overlying strata behavior during secondary gob-side entry retaining.

4.1. Development of Mechanical Model for Secondary Gob-Side Entry Retaining

The block equilibrium method is used to analyze the stability of the overlying "large structure" above the roadway. First, the magnitude and location of the support force provided by the secondary gob-side entry retaining are determined for the selected stratum, establishing a mechanical model that describes the interaction between the support system and the surrounding rock, as shown in Figure 6. To facilitate the solution process, the model is simplified as follows:

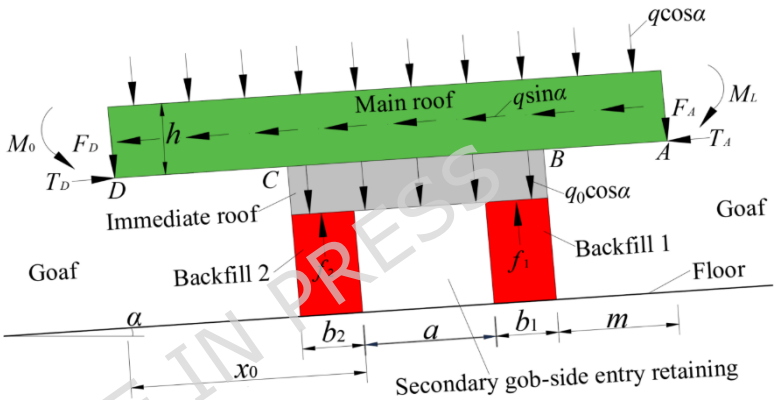

Fig. 6. Stress analysis diagram of roof fracture structure of secondary gob-side entry retaining.

(1) The weight of weak rock strata above the main roof uniformly acts on the main roof, combining with the dead weight of the main roof to create a uniformly distributed load q, and the dead weight of the immediate roof is a uniformly distributed load q_0.

(2) The immediate roof, main roof, and weak rock strata above the main roof are isolated from the strata at higher positions, and it is assumed that the shear force between the layers is 0.

(3) The characteristic dimension L_1 of strata fractures is linked to the initial weighting interval l for the main roof of the coal face and the coal face length L_m [29].

$$L_1 = \frac{l^2}{2L_m}\left[\sqrt{1+3\left(\frac{L_m}{l}\right)^2}-1\right] \tag{1}$$

$$L_3 = \frac{l}{2}\left[\sqrt{\frac{l^2}{4L_m^2}+3}-\frac{l}{L_m}\right] \tag{2}$$

In a similar simulation test of gob-side entry retaining, the main roof above the gob-side entry retaining gradually fractures with mining in the coal face, forming a "voussoir beam" structure at the end of the coal face. The main roof in the middle of the coal face fractures into multiple rectangular blocks, each with a length shorter than that of the curved triangular block at the end of the coal face. To address the most dangerous case of roadway main roof fracture, the value for L_2 should be equal to L_3.

(4) Following the fracture of the main roof at the upper section's end of the coal face, the vertical force and bending moment of key block A on key block B are F_A and M_L (ultimate fracture), respectively, with $F_A = L_1 q\cos\alpha$. After the

main roof fracture at the next section's end of the coal face, the vertical force and bending moment of key block D on key block C are F_D and M_0 (the residual bending moment of the second fracture of the main roof), respectively, with $F_D = L_2 q \cos\alpha$. The uniformly distributed loads of backfill 1 and backfill 2 in secondary gob-side entry retaining are f_1 and f_2, respectively.

(5) During gob-side entry retaining, the main roof undergoes rotation and tilting towards the goaf in the upper section, with the elastic-plastic junction in the coal wall beside the roadway serving as the rotation axis. The formulas for calculating the abutment pressure σ_y and the width x_0 of the limit equilibrium zone for the integrated coal beside the roadway are as follows [30]:

$$x_0 = \frac{MA}{2\tan\varphi_0} \ln\left(\frac{k\gamma H \cos\alpha + \frac{c_0}{\tan\varphi_0}}{\frac{c_0}{\tan\varphi_0} + \frac{p_x}{A}}\right) \tag{3}$$

Where c_0 and φ_0 denote the cohesive force (MPa) and internal friction angle (°) of the interface between coal seam and strata on the roof and floor, respectively; p_x represents the support strength (MPa) of the coal side; A denotes the lateral pressure coefficient (dimensionless); μ_m indicates the Poisson's ratio of coal (dimensionless); M represents the mining height (m); k denotes the maximum stress concentration factor (dimensionless); γ indicates the average volume weight of overlying strata (kN/m³); H denotes the mining depth (m).

(6) m denotes the cantilever length (m) of the main roof outside backfill 1, and the support resistance in secondary gob-side entry retaining is disregarded.

The above simplifications are made to render the mechanical model analytically tractable. Key assumptions include: neglecting interlayer shear, treating overlying weak strata as uniform load, and assuming planar strain conditions. These are reasonable for typical deep mining conditions where the main roof is thick and relatively continuous. However, the model may be less applicable for highly fractured or steeply dipping strata, and 3D edge effects are not considered. Future work could incorporate more sophisticated numerical models to address these limitations.

4.2. Calculation of Backfill Support Resistance

According to Figure 6, the equilibrium method is employed to formulate a mechanical equation for the composite laminate model of secondary gob-side entry retaining.

The resultant force in the direction perpendicular to strata inclination α is 0, leading to the following conclusions:

$$\begin{aligned} f_1 b_1 + f_2 b_2 = {} & q\cos\alpha \times (m + b_1 + a + x_0) + \\ & q_0 \cos\alpha \times (b_1 + a + b_2) + L_1 q \cos\alpha + L_2 q \cos\alpha \end{aligned} \tag{4}$$

For the AD block, parallel to direction α, based on $\sum T_x = 0$, the following expression can be obtained:

$$T_D = T_A + q\sin\alpha \times (m + b_1 + a + x_0) \tag{5}$$

For the strata of the immediate roof, following $\sum M_C = 0$, the resulting expression is:

$$\begin{aligned} & f_1 b_1 \times \left(\frac{b_1}{2} + a + b_2\right) + f_2 b_2 \times \frac{b_2}{2} + L_2 q\cos\alpha \times (x_0 - b_2) - \\ & L_1 q\cos\alpha \times (m + b_1 + a + b_2) + \frac{1}{2} h q \sin\alpha \times (m + b_1 + a + x_0) \\ & + \frac{1}{2} q\cos\alpha \times \left[(x_0 - b_2)^2 - (m + b_1 + a + b_2)^2\right] - \\ & \frac{1}{2} q_0 \cos\alpha \times (b_1 + a + b_2)^2 + M_0 - M_L = 0 \end{aligned} \tag{6}$$

Where a denotes the roadway width; b_1 and b_2 represent the width of backfill 1 and backfill 2, respectively; h indicates the thickness of the rock strata on the main roof.

Combining equations (4) and (6), the system of linear equations with two unknowns is solved as follows:

$$\begin{aligned} f_1=\{&q\cos\alpha\times[(m+b_1+a+b_2)^2-(x_0-b_2)^2-(m+b_1+a+x_0)b_2\\ &+L_1(2m+2b_1+2a+b_2)-L_2(2x_0-b_2)]-hq\sin\alpha(m+b_1+a+x_0)\\ &+q_0\cos\alpha\times[(b_1+a+b_2)^2-(b_1+a+b_2)b_2]+2(M_L-M_0)\}/\\ &(b_1+2a+b_2)b_1 \end{aligned} \tag{7}$$

$$f_2=[q\cos\alpha\times(m+b_1+a+x_0+L_1+L_2)+ q_0\cos\alpha\times(b_1+a+b_2)-f_1b_1]/b_2 \tag{8}$$

4.3. Influencing Factors Analysis of Surrounding Rock Stability for Secondary Gob-Side Entry Retaining

According to Formula (1)–(4), once the mining depth H, coal face width L_m, mining height M, and initial weighting l of the main roof are determined, considering roadway support, the roadway width a, the width b_1 of backfill 1, the width b_2 of backfill 2, and the cantilever length m of the main roof on the side of the goaf are reduced. Simultaneously, the support strength p_x of the coal wall beside the roadway is improved, aiming to further decrease the width x_0 of the limit equilibrium zone and alleviate the load on the two filling bodies. This strategy ultimately eases the pressure on the roadway surrounding rock.

Referring to Formula (5), the stability of the roadway roof strata is contingent upon the horizontal force T_D provided by key block D when the dip angle of the coal seam α is determined. If T_D falls short of the resultant force of the component force $q\sin\alpha(m+b_1+a+b_2+x_0)$ of the road roof strata and T_A, the roadway roof may tilt toward the goaf in the next section, potentially causing instability. Therefore, minimizing m, b_1, a, b_2, x_0 can weaken the force T_A applied by key block B, contributing to the stability of the roadway roof.

As per Formula (7) and (8), f_1 and f_2 are interconnected. The greater the support resistance of backfill 1, the smaller the support resistance required by backfill 2, and vice versa. Hence, when determining the support resistance of backfill 2 in gob-side entry retaining, one should also consider its impact on the support resistance of backfill 2 in secondary gob-side entry retaining.

5. Engineering Practice

The 52210 working face is located in a deep coal mine with an average depth of 610 m. The immediate roof consists of sandy mudstone (2-4 m thick), followed by a main roof of fine sandstone (8-12 m thick). The coal seam thickness is 1.8 m with a dip angle of 17°. The floor is composed of mudstone and sandy mudstone (4-6 m thick). Similar simulation tests and field measurements were conducted prior to the design to obtain key parameters such as initial weighting interval and overburden load.

5.1. Determination of Support Parameters for Backfill

Based on the actual geological conditions of the section drift in the 52210 coal face of a certain mine, along with similar simulation test results and measured field data, the necessary parameters for calculation are derived as follows: H=610 m，α=17°，L_m=125 m，l=35 m，a=4.4 m，M=1.8 m，P_x=0.35 MPa，m=2 m (reflecting the pre-splitting blasting outcome of deep holes in the roadway roof), A=0.4，k=3，φ_0=26°，γ=24 kN/m^3，c_0=1.5 MPa，μ_m=0.2，q=1.02 MPa，q_0=0.06 MPa，h=4 m，M_0=M_L (considering the most hazardous scenario in secondary gob-side entry retaining). Utilizing Formulas (7) and (8), the relationship between roadway-side support resistance f_1, f_2 and b_1, b_2 is obtained, as depicted in Figure 7.

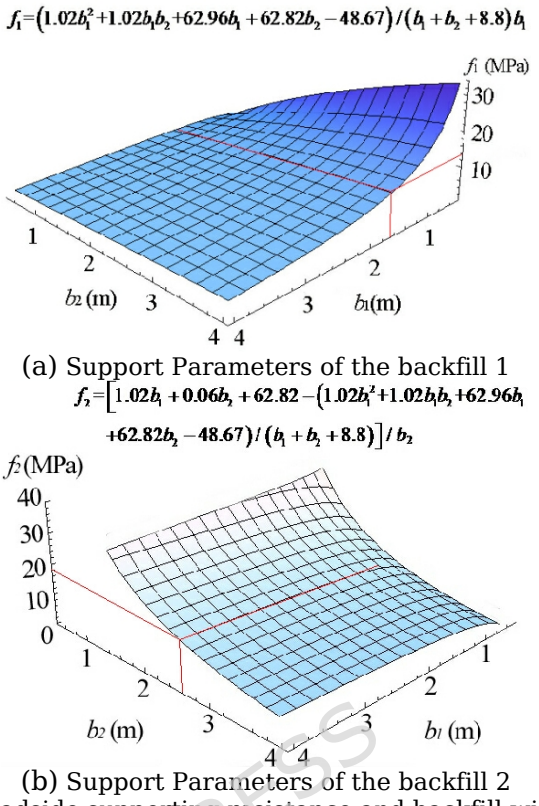

Fig. 7. Relation of roadside supporting resistance and backfill width.

From Figure 7, when $b_1 \geq 1.6$ m and $b_2 \geq 2.5$ m, $f_1 \leq 10.46$ MPa and $f_2 \leq 19.15$ MPa. These threshold widths were selected based on a trade-off between material economy and mechanical safety: Narrower widths would demand excessively high strength, while wider ones would increase material cost without significantly reducing required resistance. The chosen values also align with the available filling equipment and space constraints in the mine. Consequently, the subsequent support scheme adopts b_1=1.6 m and b_2=2.5 m m as design bases.

5.2. Supporting Scheme of Secondary Gob-Side Entry Retaining

Due to the strong mining influence experienced by secondary gob-side entry retaining and its extended service life, it has been determined through research that the return airway of the 52210 working face will adopt a combined support scheme consisting of bolt-cable-mesh, U-shaped steel sets, and grouting with shotcrete. The specific support parameters are illustrated in Figure 8. The systematic linkages between the key support parameters and the four coordination objectives of the “four-in-one” system are presented in Table 1.

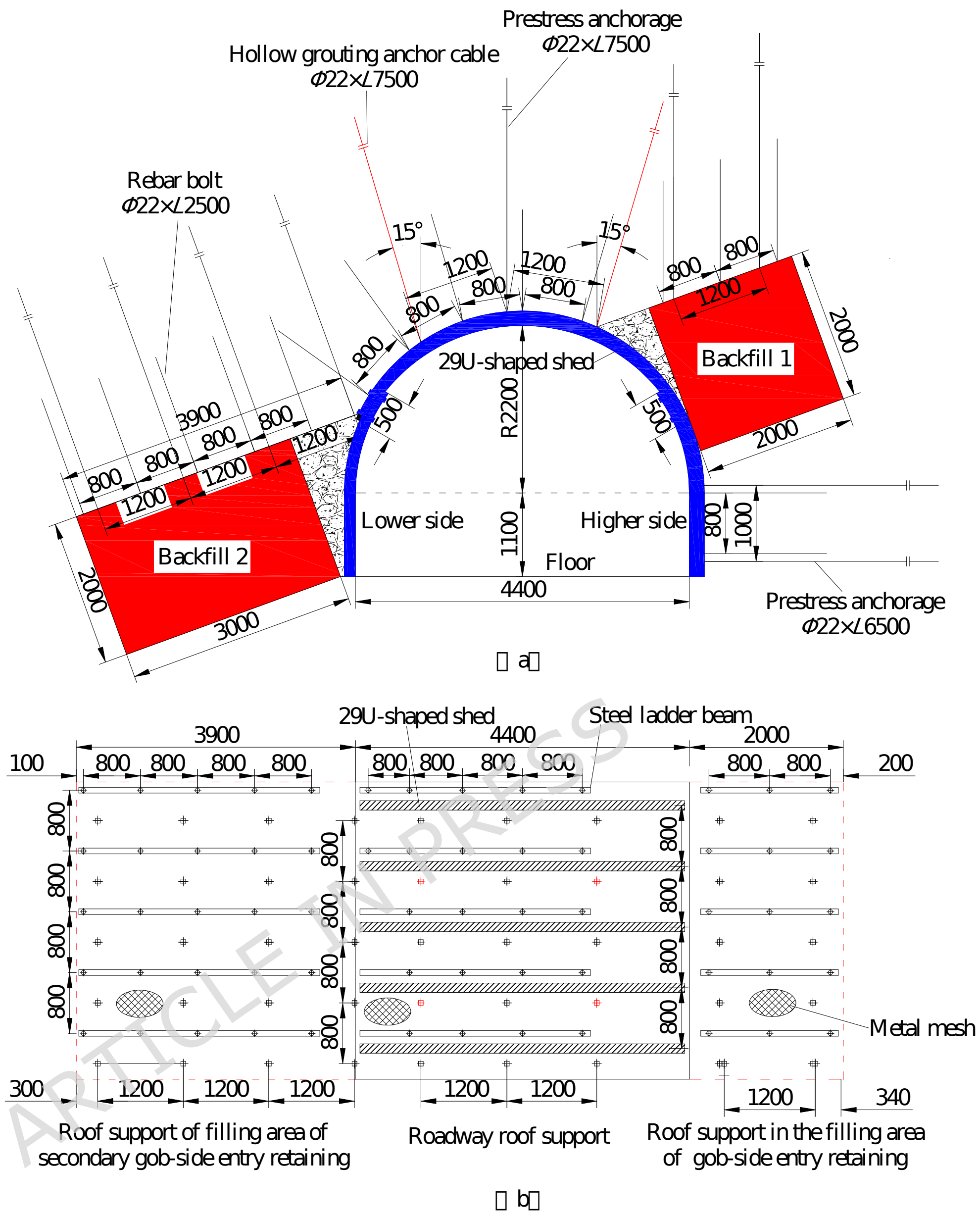

Fig. 8. Support scheme of secondary gob-side entry retaining. (a) Sectional view of support scheme of secondary gob-side entry retaining. (b) Vertical view of roof support scheme of secondary gob-side entry retaining.

Coordination objective	**Relevant components**	**Main measure**
Coordinated roof support	Roof bolts, cables, grouting	High-density bolting, long cables, roof grouting
Roof-floor-backfill interaction	Backfill material, floor reinforcement	Backfill ucs: 32-36 MPa
Coordinated bearing between backfills	Dual backfill bodies	Widths: b_1=1.6 m, b_2=2.5 m Strength ratio: f_2□f_1
Roadway support and backfill interaction	Internal support, steel sets	Hydraulic props, U29 arches

Table 1. Linkages between key support parameters and the four coordination objectives of the "four-in-one" system.

(1) Roadway support parameters

The roadway roof support system consists of: The threaded steel bolts (Φ22 mm×2,500 mm) installed in a pattern of 5 bolts per row with 3.6 m-long 14# steel ladder beams and 10 # metal mesh, having a spacing of 800 mm between bolts and 800 mm between rows. The prestressed cable bolts (Φ22 mm×7,500 mm) arranged in a "3-1-3-1" pattern with 1,200 mm spacing and 800 mm row spacing, where the central cable is offset 200 mm to the right and installed vertically while the others are angled 15° outward. The groutable hollow cable bolts (Φ22 mm×7,500 mm) installed in a "2-0-2-0" configuration with 2,400 mm spacing and 1,600 mm row spacing, all angled 15° outward. The U29 steel arch supports spaced at 800 mm intervals, forming a comprehensive support structure designed to ensure roof stability under mining-induced stresses.

The lower side of the roadway high side employs: The threaded steel bolts (Φ22 mm×2,500 mm) installed vertically in pairs per row with 10 # metal mesh, featuring 800 mm spacing between bolts and 800 mm row spacing, all arranged horizontally. The prestressed cable bolts (Φ22 mm×6,250 mm) with 1,200 mm spacing and 1,000 mm row spacing, where two parallel rows of cable bolts are installed along the roadway axis and reinforced with 2 m-long 14# channel steel for additional strengthening.

(2) Roof support scheme of filling area

The roof support parameters of backfill area for the gob-side entry retaining (located more than 6 m ahead of the working face where a notch is excavated in the coal wall at the panel end) consist of: Threaded steel bolts (Φ22 mm×2,500 mm) installed vertically in rows of 3 bolts each with 2.0 m-long 14 # steel ladder beams and 10 # metal mesh, having 800 mm spacing between bolts and 800 mm row spacing. Vertically installed prestressed cable bolts (Φ22 mm×7,500 mm) arranged with 1,200 mm spacing and 800 mm row spacing, forming a reinforced support system specifically designed for the entry retaining section adjacent to the excavated notch.

The roof support parameters for the secondary gob-side entry retaining backfill area consist of: Five threaded steel bolts per row with 3.4 m long 14 # steel ladder beams and 10# metal mesh, installed perpendicular to the roof strata with 800 mm spacing between bolts and 800 mm row spacing. Three cable bolts per row arranged perpendicular to the roof strata with 1,200 mm spacing and 800 mm row spacing, forming an optimized support system specifically designed for the secondary mining impact conditions.

(3) Initial reinforcement support of gob-side entry retaining

For both initial and secondary gob-side entry retaining operations, immediate internal roadway reinforcement should be implemented, particularly within 150 m behind the working face. This is typically achieved using single hydraulic props with 400 mm×400 mm base plates, arranged in 1-3 rows along the roadway axis for enhanced support.

(4) Pre-mining reinforcement for secondary gob-side entry retaining

To enhance the grouting effectiveness of hollow groutable cable bolts and prevent grout leakage during injection, shotcrete should be applied to the roadway surrounding rock with a minimum thickness of 100 mm and strength grade of C20. Subsequently, roof grouting reinforcement is conducted with the following parameters: using P.O 42.5 ordinary Portland cement, with a water-cement ratio of 0.8:1 to 0.75:1 for single-fluid grout, or adding sodium silicate solution at 45 Bé (comprising 3%-5% of cement weight) for two-fluid grout. The grouting pressure should be maintained at 2-3 MPa with a stabilization time of 3-5 minutes.

(5) Roadway side support

The roadway side filling operation utilizes specialized coal mine backfill material composed of Portland cement (P.O 42.5), fly ash (Grade I), medium sand (fineness modulus 2.6-3.0), water (PH 6.5-8.5) and chemical additives (1.2-1.8% by weight). This engineered composite demonstrates superior cost-effectiveness and mechanical performance, achieving initial compressive strength of 5-8 MPa within 8 hours and final strength of 32-36 MPa at 28 days. The filling system incorporates a Φ18 mm rebar framework (300 mm×300 mm grid) with 50 mm concrete cover, enhancing its uniaxial compressive strength (UCS) to 42±2 MPa and shear resistance to 15±1 MPa, effectively mitigating potential rotational displacement (≤3 mm) towards the goaf area during periodic weighting.

To reduce the cantilever length of the main roof above the retained entry, deep-hole pre-splitting blasting was conducted in the roof strata outside the backfill zones. This technique promotes controlled fracturing and encourages complete caving of the roof beyond the backfill, thereby shortening the effective cantilever length. In the 52210 face, blasting holes (diameter 75 mm, depth 10-12 m) were drilled at an angle outward from the roadway, with charges placed every 2 m. Detonation was timed with face advance to ensure timely roof collapse.

5.3 Surrounding Rock Observation of Roadway

A comprehensive strata pressure monitoring program was implemented throughout the secondary gob-side entry retaining process in Panel 52210, focusing on: fracture development patterns in roof strata; surrounding rock deformation behavior; load-bearing capacity distribution within backfill structures during both initial and secondary gob-side entry retaining phases.

The observation station layout of secondary gob-side entry retaining was shown in Figure 9, which mainly included: Three borehole inspection points per cross-section to map fracture zones (broken/frac-tured regions) based on crack propagation analysis. Six displacement stations (roof-floor + rib-to-rib) spaced at 30 m intervals for monitoring pre-/post-face deformation characteristics. Four embedded stress cells in each backfill (phase I/II) to record stress evolution ahead/behind the working face. This tripartite monitoring system captured key mechanical responses: fracture networks extending 2.8-3.5 m into roof strata, asymmetric displacement (max 387 mm at vulnerable zones), and dynamic stress transfer (peak 18.6 MPa) within backfill structures.

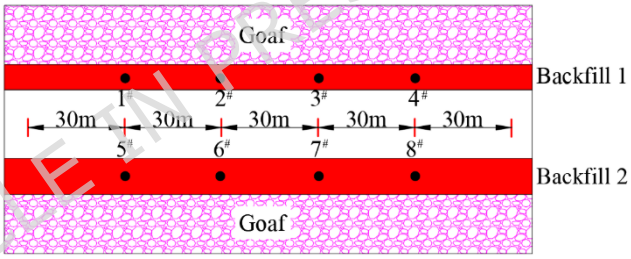

Fig. 9. Observation station layout of secondary gob-side entry retaining.

(1) Development characteristics of roof fractures

To gain deeper insight into roof failure mechanisms during secondary gob-side entry retaining, borehole endoscopic inspection was conducted, with the resulting roof fracture development patterns illustrated in Figure 10. The imaging observation results of the borehole viewer indicate that within the central anchored zone of the secondary gob-side entry retaining roof, fracture development is minimal with limited damage extent (within 1 m). However, pronounced deep fractures (beyond 5 m) are observed in bilateral roof areas (particularly on the low-side roof section), while shallow fractures remain underdeveloped. This fracture pattern indicates favorable shear-sliding and fracturing along the exterior boundaries of both backfill bodies, which contributes positively to roadway stability.

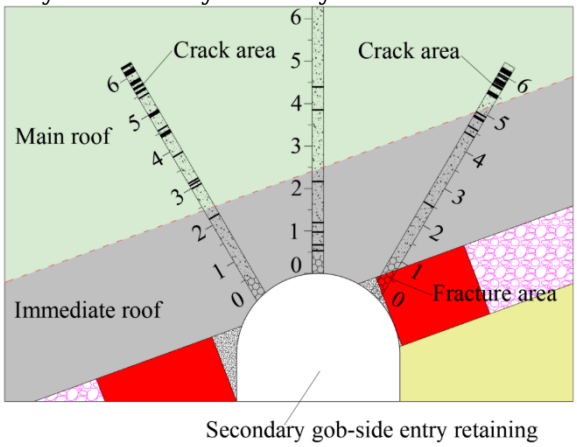

Fig. 10. Development state of roof fracture of secondary gob-side entry retaining.

(2) Backfill load analysis

Based on the measured data from hydraulic pressure cells embedded within the backfill structure, Figure 11 illustrates the evolution pattern of backfill loading in relation to face advance distance.

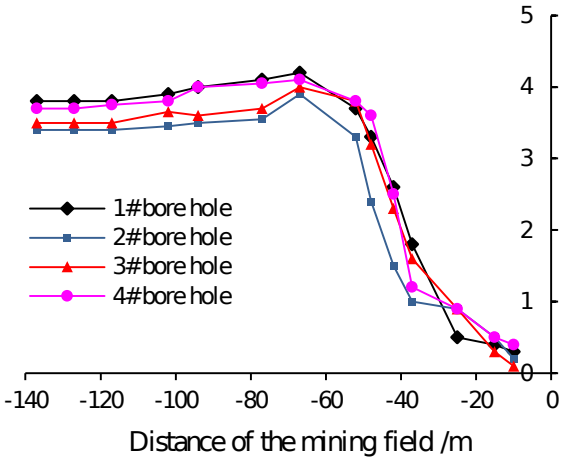

(a) Load distribution characteristics of the backfill 1 of gob-side entry retaining

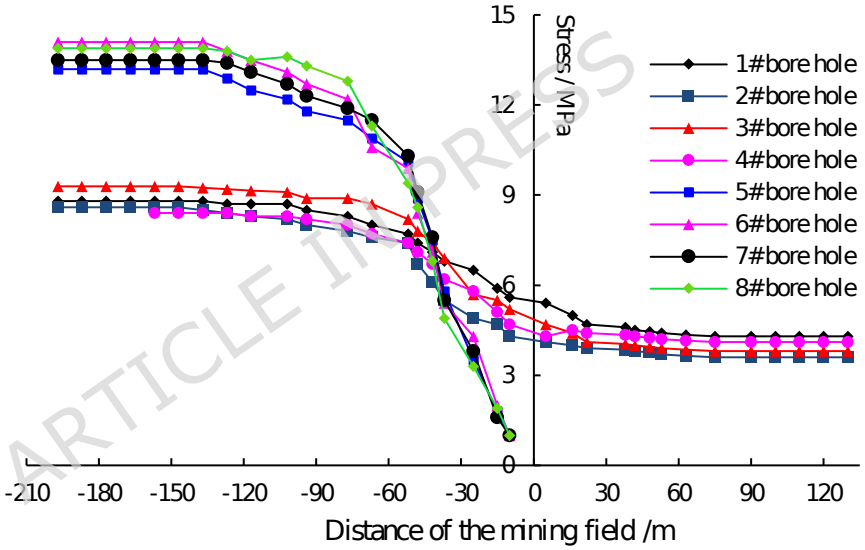

(b) Load distribution characteristics of the backfill 2 of secondary gob-side entry retaining

Fig. 11. Load evolution characteristics of two backfills.

As depicted in Figure 11(a), during the gob-side entry retaining process, Backfill 1 exhibits a three-stage loading characteristic: A sharp load increase within 0-50 m behind the working face; A decelerated load rise between 50-70 m; A stabilization phase beyond 70 m where the load eventually reaches a steady-state value of 4.0 MPa, reflecting complete stress equilibrium in the surrounding rock mass.

As illustrated in Figure 11(b), during secondary gob-side entry retaining, Backfill 1 maintains remarkable stability with minimal load fluctuations within 100m ahead of the working face. Behind the face, both backfill bodies undergo synchronized but differential loading behavior: Rapid stress escalation (0-70 m) where Backfill 2 demonstrates 1.5 times faster loading rate; Progressive load deceleration (70-130 m); Ultimate stabilization (>130 m) with distinct final loads 9.7 MPa for Backfill 1 and 13.9 MPa for Backfill 2, representing a 43% higher bearing capacity requirement for the secondary backfill structure.

The differential loading arises because Backfill 2 bears not only the weight of key block C but also additional transfer from the already-stressed Backfill 1 and the overlying strata disturbed by secondary mining. This aligns with the mechanical model prediction that $f_2 > f_1$ under secondary retaining conditions. The observed fracture pattern—deep vertical cracks near backfill edges—

facilitates shear transfer to the backfills, helping key block C remain stable through horizontal thrust.

(3) Deformation behavior of roadway surrounding rock

During the initial gob-side entry retaining phase, Figure 12(a) demonstrates that as the upper panel working face advances: The mining-induced disturbances progressively intensify when approaching within approximately 60 m ahead of the face; The rapid deformation occurs 0-70 m behind the face; A moderated deformation phase follows at 70-100 m before stabilization. The cumulative displacements ultimately reach: low-side displacement 227 mm, high-side 19 mm, roof settlement 101 mm, and floor heave 336 mm, revealing significant asymmetric behavior with predominant floor failure.

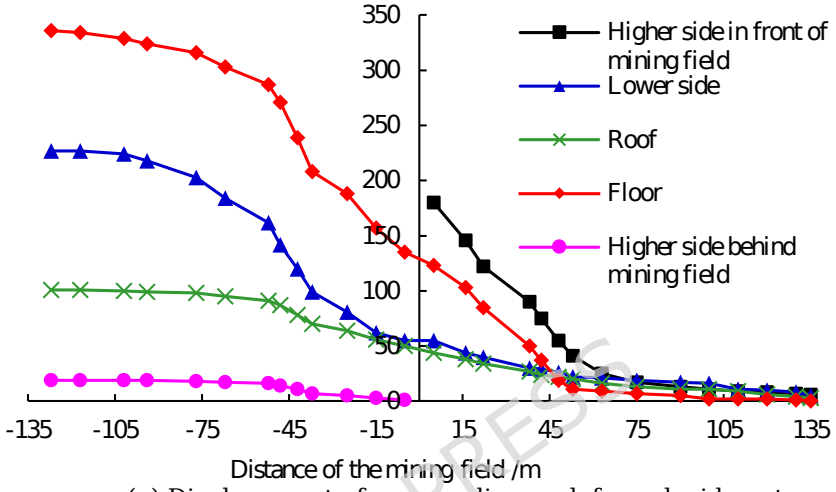

(a) Displacement of surrounding rock for gob-side entry retaining

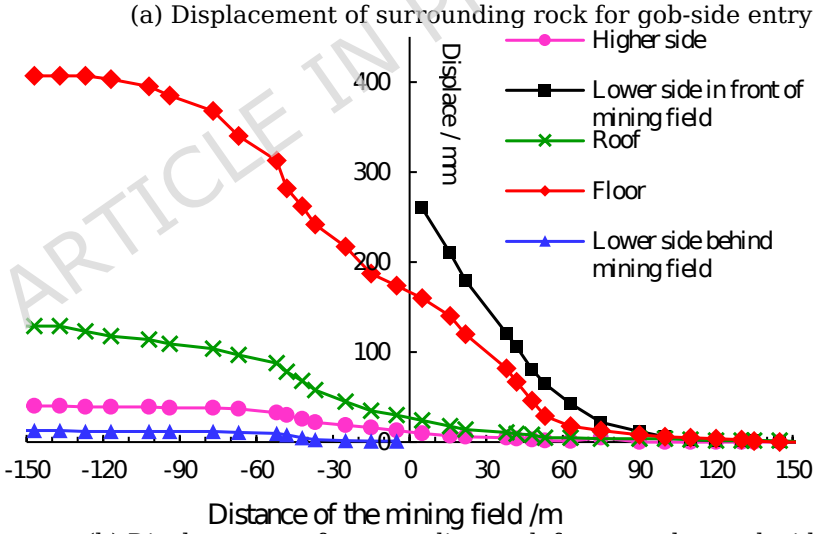

(b) Displacement of surrounding rock for secondary gob-side entry retaining

Fig. 12. Displacement of surrounding rock.

During the secondary gob-side entry retaining phase, Figure 12(b) reveals: Mining-induced disturbances commence at approximately 80 m ahead of the working face, with progressively increasing surrounding rock displacement; The deformation moderation period occurs 90-120 m behind the face before stabilization. Final cumulative displacements measure: high-side displacement 13 mm, low-side 40 mm, roof settlement 129 mm, and floor heave 407 mm.

Fig. 13. Maintenance effect of secondary gob-side entry retaining.

These results demonstrate that post-stabilization: The roof and rib deformations remain controlled (<150 mm); The excessive floor heave necessitates remedial grading (average 380 mm cutting depth required); The overall maintenance effectiveness is validated in Figure 13 through roadway serviceability metrics; The substantial floor heave indicates that floor control, though implemented, may be insufficient under the high asymmetric loads transferred via the backfills. Potential refinements include increasing grouting depth, using stronger floor bolts, or installing invert arches. The current strategy relied on shotcrete and shallow grouting; deeper reinforcement or structural floor supports could be considered in future designs.

Based on a comprehensive analysis, it is concluded that during the secondary gob-side entry retaining stage, both the extent and intensity of roadway surrounding rock deformation are significantly greater and more prolonged than during the initial retaining stage, especially in the zones ahead of and behind the working face. The primary cause of severe roadway deformation is the intense overlying strata movement triggered by the first and periodic weighting of the main roof behind the working face. These dynamic pressure effects are most pronounced during secondary gob-side entry retaining operations.

It should be noted that this study proposes an innovative support strategy specifically designed for secondary gob-side entry retaining in thin coal seams. While the proposed method has demonstrated effectiveness in controlling surrounding rock deformation, further research is still needed to develop simpler, more economical, and equally efficient alternatives—particularly in terms of implementability and cost optimization—and to achieve a better balance between support performance and operational efficiency under complex mining conditions.

6. Conclusions

(1) The study clarifies the overlying strata movement behavior throughout the entire process of secondary gob-side entry retaining, showing that the “macro-structure” of the overlying strata undergoes three distinct adjustment phases before reaching stability. Through a systematic analysis, the research identifies and characterizes the critical key blocks that dominate the stability of the surrounding rock in secondary gob-side entry retaining.

(2) The supporting “micro-structure” in secondary gob-side entry retaining comprises four integral components: The roof strata, dual backfill bodies (including both the primary and secondary gob-side entry retaining walls), the floor strata, and the internal roadway support system. Based on a comprehensive analysis of the load-bearing behavior and interaction mechanisms of each component, this study proposes an innovative “four-in-one” surrounding rock control methodology specifically developed for secondary gob-side entry retaining.

(3) This study establishes a mechanical model for the overlying strata structure in secondary gob-side entry retaining and systematically analyzes the factors influencing surrounding rock stability. The results show that when mining depth, panel width, and extraction height are predetermined, strategically reducing three key parameters—roadway width, backfill width, and the cantilever length of the main roof above the retained entry—can significantly improve the load-bearing capacity of the solid coal rib during the

initial gob-side entry retaining stage. This in turn reduces the operational load on the two backfill bodies during the secondary gob-side entry retaining stage, thereby effectively alleviating surrounding rock pressure.

(4) The surrounding rock control in secondary gob-side entry retaining poses significant engineering challenges. Although field observations confirm that the overlying strata structure maintains relative integrity during secondary gob-side entry retaining operations, the implementation of support systems remains technically demanding due to complex stress redistribution. This highlights the need for further research to develop more comprehensive support theories and optimized control strategies specifically for secondary gob-side entry retaining, particularly regarding the interaction mechanisms between the dual backfill bodies and the composite roof structure.

Data availability

The datasets generated or analyzed during the current study are available from the corresponding author on reasonable request.

References

1. Ming, C.; He, M.C.; Wang, J.; Liu, J.N.; Coli, M. Control technology of surrounding rock stability based on compensation theory in gob-side entry retaining with composite hard roof. *Journal of Mountain Science*, **22**(03): 1029-1047 (2025).
2. Zhu, H.Z.; Xu, L.; Wen, Z.J. Ground response and failure mechanism of gob-side entry by roof cutting with hard main roof. *Journal of Central South University*, **31**(07): 2488-2512 (2024).
3. Zheng, L.J.; Wang, W.; Zhang, G.J. Study on the technology of gob-side entry retaining by roof cutting to release pressure in fully mechanized mining working face with high stress. *Journal of Henan Polytechnic University (Natural Science)*, **40**(06): 43-53 (2021).
4. Zhang, Z.Z.; Deng, M.; Bai, J.B.; Yan, S.; Yu, X.Y. Stability control of gob-side entry retained under the gob with close distance coal seams. *International Journal of Mining Science and Technology*, **31**(02): 321-332 (2021).
5. Jia, H.S.; Wang, Y.B.; Wang, W.J.; Yao, Q.L.; Liu, S.W.; Li, C.; Peng, B.; Zhang, Z.P.; Mi, Z.W. Bearing characteristics of brokenstone columnin goaf of large dip angle coal seam and stability mechanism of gob-side entryretaining. *Journal of China University of Mining □ Technology*, **54**(03): 595-608 (2025).
6. Wang, J.; Liu, P.; Jiang, J; Sun, Z. Y-shaped ventilation air leakage law of working face of gob-side entry retaining by cutting roof to release pressure. *Journal of Mining* & *Safety Engineering*, **38**(03): 625-633 (2021).
7. Li, Y.F.; Hua, X.Z. Mechanical analysis on the stability of surrounding rock structure of gob-side entry retaining. *Journal of China Coal Society*, **42**(09): 2262-2269 (2017).
8. Chen, Y.; Yang, Y.G.; Yan, S.; Hao, S.P.; Cao, Q.J. Study on reinforcement mechanism of filling body in gob-side entry retaining. Journal of Mining & Safety Engineering, **35**(06): 1129-1134 (2018).
9. Kan, J.G.; Wu, J.K.; Zhang, N.; Liang, D.X. Structure stability analysis and control technology of surrounding rock of the secondary gob-side entry retaining. *Journal of Mining* & *Safety Engineering*, **35**(05): 877-884 (2018).
10. Wang, Q.;He, M.C.; Yang, J. Study of a no-pillar mining technique with automatically formed gob-side entry retaining for longwall mining in coal mines. *International Journal of Rock Mechanics and Mining Sciences*, 110: 1-8 (2018).
11. Han, C.L.; Zhang, N.; Ran, Z.; Gao, R.; Yang, H.Q. Superposed disturbance mechanism of sequential overlying strata collapse for gob-side entry retaining and corresponding control strategies. *Journal of Central South University*, **25**(09): 2258-2271 (2018).
12. Wang, Z.C.; Li, W.; Bi, L.P.; Qiao, L.P.; Liu, R.C.; Liu, J. Estimation of the REV size and equivalent permeability coefficient of fractured rock masses with an emphasis on comparing the radial and unidirectional flow configurations. *Rock Mechanics and Rock Engineering*, **51**(05): 1457-1471 (2018).
13. Liu, Q.S.; Lei, G.F.; Peng, X.X.; Lu, C.B.; Wei, L. Rheological characteristics of cement grout and its effect on mechanical properties of a rock fracture. *Rock Mechanics and Rock Engineering*, **51**(02): 613-625 (2018).
14. Dou, L.M.; He, H. Study of OX-F-T spatial structure evolution of overlying strata in coal mines. *Chinese Journal of Rock Mechanics and Engineering*, **31**(03): 453□460 (2012).
15. Xin, Y.J.; Tian, M.H.; Ji, H.Y.; Zhang, D.Y.; Gao, Z.G.; Ren, J.W.; Zhao, K. Collaborative bearing mechanism of support body-accumulation body along gobfor

gob-sideretention gateway. *Journal of China University of Mining* & *Technology*, **54**(03): 595-608 (2025).
16. Zhang, Z.Z.; Bai, J.B.; Wang, X.Y.; Xu, Y.; Yan, S.; Liu, H.L.; Wu, W.D.; Zhang, W.G. Review and development of surrounding rock control technology for gob-side entry retaining in China. *Journal Of China Coal Society*, **48**(11): 3979-4000 (2023).
17. Zhang, Z.Z.; Bai, J.B.; Wang, W.J.; Chen, Y.; Yu, X.Y.; Wu, H. Mechanical analysis of roof separation within and outside anchorage zone above backfill area of gob-side entry retaining and its engineering application. *Journal of Mining* & *Safety Engineering*, **35**(05): 893-901 (2018).
18. Zhang, Z.Z.; Wang, W.J.; Chen, Y.; Yu, X.Y. Study on stress state of immediate roof above backfill area ingob-side entry retaining and its application. *Journal of China Coal Society*, **42**(08): 1960-1970 (2017).
19. Deng, X.J.; Dong, C.W.; Yuan, Z.X.; Zhou, N.; Yin, W. Deformation behavior of gob-side filling body of gob-side retaining entry in the deep backfilling workface. *Journal of Mining* & *Safety Engineering*, **37**(01): 62-72 (2020).
20. Feng, G.R.; Ren, Y.Q.; Wang, P.F.; Guo, J.; Qian, R.P.; Li, S.Y.; Sun, Q.; Hao, C.L. Stress distribution and deformation characteristics of roadside backfill for gob-side entry of fully-mechanized caving in thick coal seam. *Journal of Mining* & *Safety Engineering*, **36**(06): 1128-1136 (2019).
21. Tang, F.R.; Ma, Z.G.; Yang, D.W.; Qi, F.Z.; Hu, J.; Chen, Y.H. Study on key parameters of filling gob-side roadway in the thick layer soft rock fault top. *Journal of Mining* & *Safety Engineering*, **36**(06): 1128-1136 (2019).
22. Hu, M.M.; Zhou, H.; Zhang, Y.H.; Zhang, C.Q.; Gao, Y.; Hu, D.W.; Li, Z. Analysis of supporting resistance of reserved pier column for gob-side entry retaining in wide roadway. *Rock and Soil Mechanics*, **39**(11): 4218-4225 (2018).
23. Sun, G.J.; Zhang, Y.; Chang, X.L.; Xin, Y.J. Technology of partition support by cutting-roof pressure relief and constant resistance reinforcement for double-used roadway with deep excavation-induced damage zone. *Journal of Mining and Strata Control Engineering*, **4**(04): 043027 (2022).
24. Han, C.L.; Zhang, N.; Ran, Z.; Gao, R.; Yang, H.Q. Superposed disturbance mechanism of sequential overlying strata collapse for gob-side entry retaining and corresponding control strategies. *J. Cent. South Univ.*, **25**: 2258-2271 (2018).
25. Wang, C.; Li, X.F.; Xiong, Z.Q.; Wang, C.; Su, C.D.; Zhang, Y.H. Experimental study on the effect of grouting reinforcement on the shear strength of a fractured rock mass. *Plos One*, **14**(08): 1−13 (2019).
26. Feng, G.R.; Ma, Z.J.; Wu, W.D.; Bai, J.B.; Du, S.W.; Bai, J.W.; He, L.J. Research on the mechanism of grouped collapse of thick and hard roof for gob-side entry retaining combined backfill in fully mechanized caving face. *Journal of China Coal Society*: 1-20 (2025).
27. Jia, H.S.; Wang, Y.B.; Wang, W.J.; Yao, Q.L.; Liu, S.W.; Li, C.; Peng, B.; Zhang, Z.P.; Mi, Z.W. Bearing characteristics of brokenstone columnin goaf of large dip angle coal seam and stability mechanism of gob-side entryretaining. *Journal of China University of Mining* & *Technology*, **54**(03): 561-576 (2025).
28. Liu Z.; Liu P.; Luo C.; Gao F.L.; Huang X.K.; Chen Z. Optimization analysis of layered materials of composite filling body beside gob-side entry retaining. *Coal Science and Technology*, **52**(10): 21-32 (2024).
29. Li, C.Y.; Gao, Y.G.; Chen, J.; Cui, X.M.; Cai, H.B. Surrounding rock stabilization and deformation evolution of gob-side entry retaining in deep colliery with mega-height coal seam extracted. *Chinese Journal of Underground Space and Engineering*, **17**(03): 897-908 (2021).
30. Gao, K.; Liu, Z.G.; Liu, J.; Deng, D.S.; Gao, X.Y.; Kang, Y.; Huang, K.F. Application of deep borehole blasting to gob-side entry retaining forced roof caving in hard and compound roof deep well. *Chinese Journal of Rock Mechanics and Engineering*, , **32**(08): 1588□1594 (2013).

Author Contributions

Conceptualization, W.J. and C.J.; methodology, W.J. and X.F.; validation, C.J. and X.F.; investigation, W.J., C.J. and X.F.; data curation, W.J.; writing—original draft, W.J.; writing—review and editing, C.J.; supervision, C.J. and X.F.; project administration, W.J.; funding acquisition, W.J. All authors have read and agreed to the published version of the manuscript.

Funding

This study was financially supported by the Science Fund Project of the National Natural Science Foundation of China (51804129); Jiangsu Postdoctoral Research Funding Program (2019K139); and National-Level Pre-research Project of Suzhou City University (2024SGY017).

Declarations

The authors declare no competing interests.

Additional information

Correspondence and requests for materials should be addressed to J.W.